Analysis of Dielectrophoretic Movement of Cell Flowing in Micro-Channel Related to Shape of Cell

Shigehiro HASHIMOTO
Biomedical Engineering, Department of Mechanical Engineering, Kogakuin University
shashimoto@cc.kogakuin.ac.jp Tokyo, 163-8677, Japan

Ryuya ONO
Biomedical Engineering, Department of Mechanical Engineering, Kogakuin University
Tokyo, 163-8677, Japan

ABSTRACT[1]

Dielectrophoresis has been tried to be applied to cell sorting technology in previous studies. In the present study, the movement of mouse myoblast cells flowing through the perpendicular electric field in a micro-channel has been analyzed *in vitro*. A pair of asymmetric surface electrodes of titanium was manufactured by the photolithography technique: a triangular electrode with the tip angle of 0.35 rad, and a rectangular electrode with the flat edge as the reference. The cyclic alternating electric current of the square wave with the period of 0.3 μs was introduced between the surface electrodes to induce the asymmetric electric field perpendicular to the main flow direction. The suspension of cells (C2C12: mouse myoblast cell line) was injected into the flow channel, and the flow rate was controlled by the pressure head between the inlet and outlet. The velocity of each cell related to the shape and alignment is measured. Experimental results show that the velocity change near the tip of the electrode is lower for a highly elongated cell. The maximum movement perpendicular to the main flow direction occurs when the major axis is perpendicular to the main flow direction.

Keywords: Biomedical Engineering, Dielectrophoresis, Flow Channel, Shape Index, Surface Electrode and Myoblast.

1. INTRODUCTION

The movement of a biological cell suspended in the medium is governed by several factors: movement of the medium, viscous resistance, gravity, electric force, Van der Waals force, and affinity of surface. Various methods have been applied to control the movement of cells *in vitro*: the flow [1], the shear field [2], the filter [3], the slit [4], the magnetic field [5], the gravitational field [6], laser [7] and the electric field [8]. These methods might contribute to several applications of manipulation of cells [9]: detection of targeted cells [10], sorting of cells [11], arrangement of cells to make a tissue, and measurement of the character of cells [12].

The movement of a charged particle depends on the electric field. The effect is applied in an electrophoresis device. When a particle is exposed to a non-uniform electric field, a force acts even on a non-charged particle. The effect depends on the polarization generated in the particle. The phenomenon is called dielectrophoresis [13]. The force of dielectrophoresis depends on several parameters: the electrical property of the particle, the shape and the size of the particle [14], the electrical property of the medium, and the electric field (the amplitude and the frequency).

The dielectrophoretic force $\boldsymbol{F}$ is generated by the non-uniform electric field $\boldsymbol{E}$.

$$\boldsymbol{F} = -2\,\pi\,\varepsilon\,(d/2)^3\,\boldsymbol{E}\,\nabla\boldsymbol{E} \tag{1}$$

In Eq. (1), d is the diameter of the particle, and ε is the permittivity of the liquid.

In the present study, the movement of mouse myoblast cells flowing through a perpendicular electric field in a micro-channel has been analyzed *in vitro*.

2. METHODS

Surface Electrode

A titanium film was used for the surface electrodes (Fig. 1). Titanium was coated on the glass plate. The thickness of coating is 200 nm. The tip angle of the triangle shape of the one of the surface electrodes is 0.35 rad. The other reference electrode has a flat edge. The distance between electrodes is 0.1 mm. The shortest connecting line between electrodes is perpendicular to the flow direction. The micro flow-channel with surface electrodes was manufactured by the photolithography technique [15].

[1] The authors are grateful to Prof. Richard L. Magin for assistance in the English Editing of this article.

Flow Channel
The pattern of the electrode with the flow channel was drawn on the mask using a laser drawing system (DDB-201K-KH, Neoark Corporation, Hachioji, Japan). The thickness of the layer on the surface electrode was measured by the stylus (with 3×10^{-5} N) of the contact profilometer (Dektak XT-E, Bruker Corporation).

The upper plate of polydimethylsiloxane has holes with the diameter of 5 mm for the inlet and outlet of the suspension. The upper plate was exposed to oxygen gas in the reactive ion etching system (FA-1), and coated with Aminopropyltriethoxysilane. After ten minutes, the upper plate was adhered to the lower plate under a pressure of 0.5 N/m^2 by sandwiching between plates of poly-methyl- methacrylate. A rectangular parallelepiped channel of 18 mm long × 0.5 mm wide × 0.035 mm high is formed between the upper and lower plates. The flow channel is placed on the stage of the inverted phase-contrast microscope.

Electric Stimulation
The electric stimulation of the alternating rectangular cyclic wave (period (T) = 0.25 μs or 0.33 μs; −15 V < amplitude (Ea) < +15 V) (Fig. 1a) was generated by an electric stimulator (WS8102, TOYO Corporation). The stimulator was connected to the titanium film electrode, and the electric stimulation was applied to the medium flow. An electric resistance (R) of 2 kΩ is serially inserted between the electrode and the stimulator to measure the electric current (I < ±7.5 mA) (Fig. 1b).

Cell
C2C12 (mouse myoblast cell line originated with cross-striated muscle of C3H mouse) was used in the test. D-MEM (Dulbecco's Modified Eagle Medium) containing 10% FBS (Fetal Bovine Serum) and 1% penicillin/ streptomycin was used for the medium.

Before the flow test, the inner surface of the flow channel was hydrophilized by oxygen plasma ashing. The bovine serum albumin solution was prefilled in the flow channel, and was incubated for thirty minutes at 310 K in the incubator.

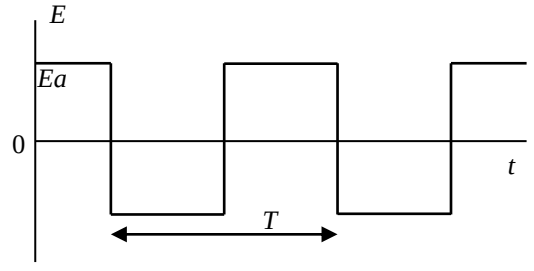

Fig. 1a: Voltage (E) tracings of rectangular wave: time (t), period (T), amplitude (Ea).

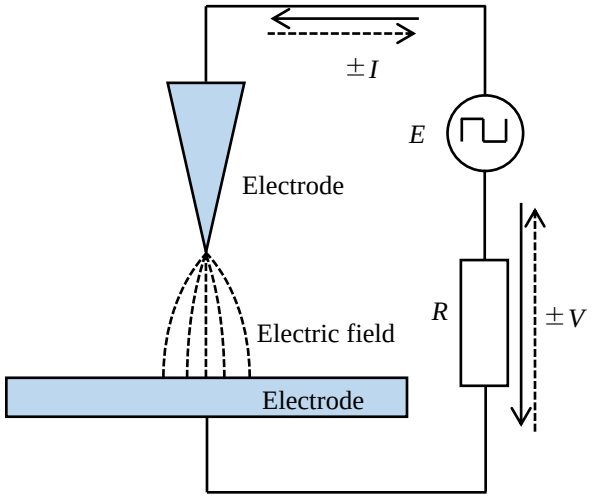

Fig. 1b: Electric circuit: alternating electric rectangular wave (E), resistance (R), voltage (V), and electric current (I).

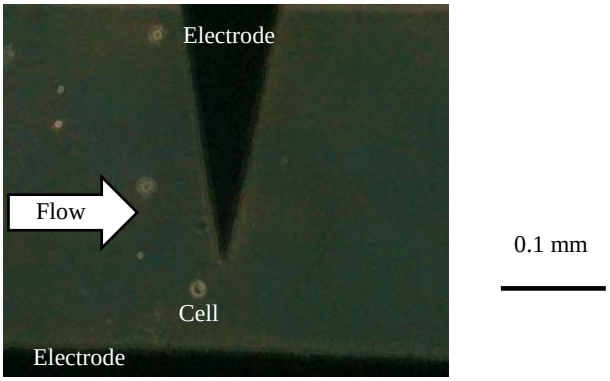

Fig. 1c: Cell passing between the electrodes in flow channel.

Before the flow test, the cells were exfoliated from the plate of the culture dish with trypsin containing EDTA (ethylenediaminetetraacetic acid), and were suspended in the medium (D-MEM: Dulbecco's Modified Eagle's Medium). The suspension of cells was poured at the inlet of the flow channel. The flow was established by the pressure difference between the inlet and outlet, which was maintained by the gravity level of the medium (< 5 mm).

Each cell passing through the flow path between the electrodes (Fig. 1c) was observed with an inverted phase-contrast microscope, and recorded with the video camera, which is placed at the eyepiece of the microscope.

Movement Analysis
The movement of the cell was analyzed by "Kinovea (Ver. 8.23, Commons Attribution)" using the video

images at 30 frames per second. To trace the movement of the cell, the coordinates are defined as shown in Fig. 1d. The main flow direction of the medium is defined as x. The perpendicular direction from the reference electrode to the tip of the triangular electrode is defined as y. Each cell makes a step-like movement near the tip of the electrode. The shifted distance (Δy) in y direction was measured by the step of the streamline of each cell. The origin is adjusted at the tip of the triangular electrode. The components (v_x, and v_y) of velocity were calculated at the tracings of each cell. The components (α_x, and α_y) of the acceleration (α) of the velocity were calculated at the velocity tracings of each cell. The maximum value of the acceleration (α_y) was picked up on each cell in Fig. 5.

The contour was approximated by an ellipse. On the ellipse, the length of the major axis (f_1), and the length of the minor axis (f_2) were measured. The ratio between axes is calculated as the shape index (f) by Eq. (2).

$$f = 1 - f_2 / f_1 \tag{2}$$

For the circle, $f = 0$. As the ellipse is elongated, f approaches to one. The angle between the major axis of each cell and the direction of the main flow (0 degrees < θ < 180 degrees) was measured. When the major axis of the cell is perpendicular to the main flow direction, θ equals 90 degrees.

In tracking of each cell, the velocity difference (Δv) is calculated by Eq (3).

$$\Delta v = v_2 - v_1 \tag{3}$$

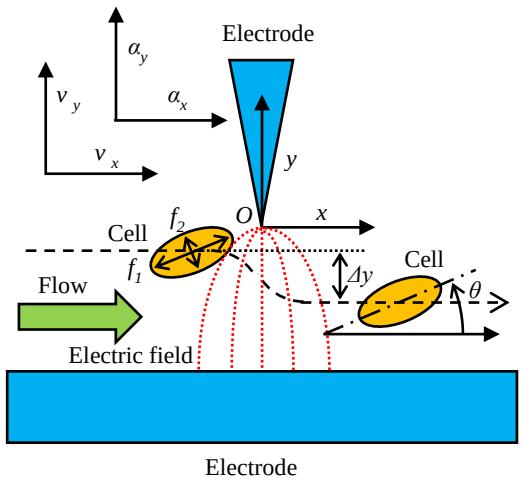

Fig. 1d: Coordinates for description of the movement of cells around and between the electrodes.

In Eq. (3), v_1 and v_2 are the mean value of v, before (v_1) and after (v_2) passing through the electric field adjacent to the tip of the electrode, respectively. The velocity differences in the x direction and in the y direction are calculated as Δv_x and as Δv_y, respectively. In tracking each cell, the acceleration difference ($\Delta\alpha$) is calculated by Eq (4).

$$\Delta\alpha = \alpha_2 - \alpha_1 \tag{4}$$

In Eq. (4), α_1 and α_2 are the mean values of α, before (α_1) and after (α_2) passing through the electric field adjacent to the tip of the electrode, respectively. The acceleration differences in the x direction and in the y direction are calculated as $\Delta\alpha_x$ and $\Delta\alpha_y$, respectively.

3. RESULTS

Fig. 2a shows the trace of each of 21 cells: under the influence of electric pulses with a period of 0.33 μs. Each cell moves stepwise around the tip of the electrode: located at the origin (x = 0, y = 0). The change of the movement in y direction is a maximum at the origin.

Fig. 2b shows the relationship between the parameters displayed in three-dimensional graph: maximum acceleration (α_{ymax}), radius (r), and initial position (y_0). The period of rectangular cyclic wave is 0.25 μs. The absolute value of the maximum amplitude of the acceleration (α_{ymax}) of the velocity of each cell during passing over the tip of the electrode is displayed in Fig. 2b. The absolute value of the maximum amplitude of the acceleration (α_{ymax}) is high, when the cell flows along the streamline (y_0 = 0) through the tip of the electrode. The absolute value of the maximum amplitude of the acceleration (α_{ymax}) by the electric field, which is perpendicular to the flow direction, increases with the radius of the cell (r).

Fig. 3 shows the relationship between the velocity and the shape index of each cell. In Fig. 3, both maximum and minimum values of the velocity during passing adjacent to the tip of the electrode are displayed. The velocities of x and y components are displayed in Figs. 3a and 3b, respectively. The component of x corresponds to the direction parallel to the main flow. The component of y corresponds to the direction perpendicular to the main flow (from the reference electrode toward the tip of the triangular electrode). The velocity of each cell fluctuated while passing through the electric field near the tip of the electrode. The range of fluctuation tends to decrease with an increase of the shape index (Figs. 3a and 3b). The velocity v_x keeps the positive values, which correspond to the direction of the velocity along the main flow (Fig. 3a). The negative values of minimum velocity of y component correspond to the movement of the cell toward to the reference electrode (Fig. 3b). The

minimum velocity of x component tends to increase with the shape index of the cell (Figs. 3a and 3b).

Fig. 4 shows the relationship between the acceleration and the shape index of each cell. The acceleration of x and y components are displayed in Fig. 4a and in Fig. 4b, respectively. The component of x corresponds to the direction parallel to the main flow. The component of y corresponds to the direction perpendicular to the main flow. In Fig. 4, both maximum and minimum values of the acceleration during passing adjacent to the tip of the electrode are displayed.

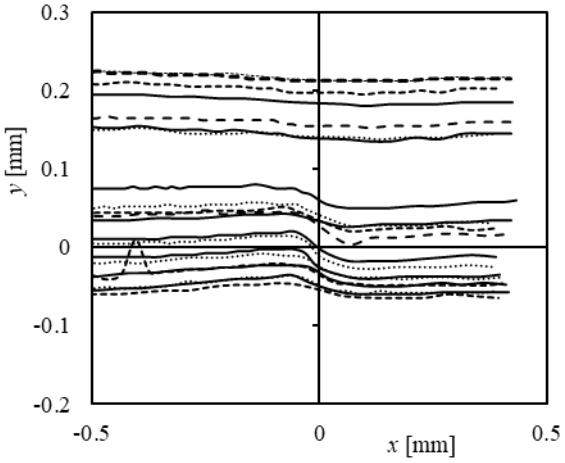

Fig. 2a: Movement of 21 cells: period of 0.33 μs.

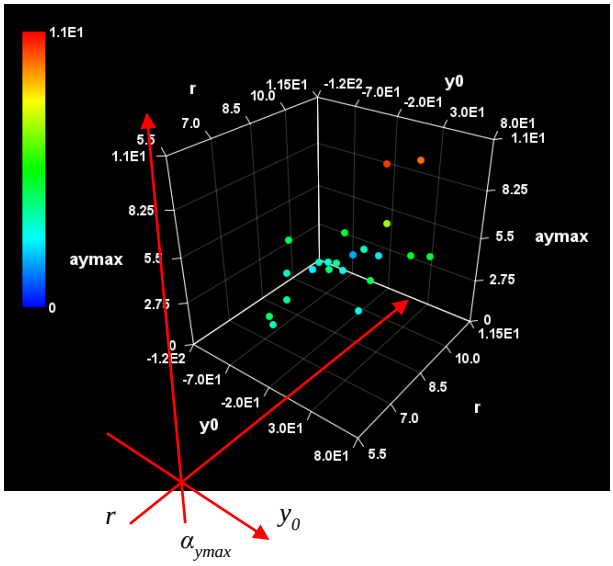

Fig. 2b: Relationship between the maximum acceleration (α_{ymax}), radius (r) , and initial position (y_0): period of 0.25 μs, amplitude of ±15 V.

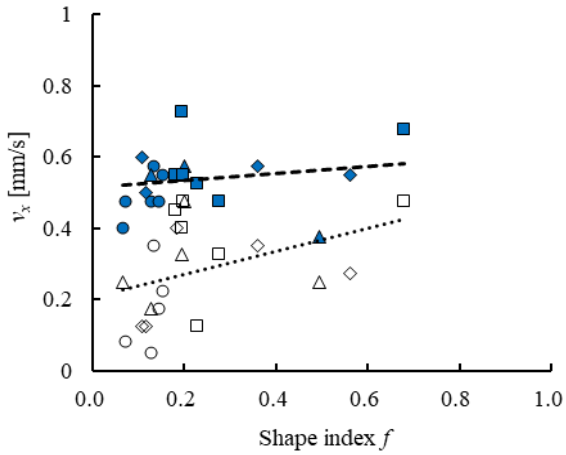

Fig. 3a: Velocity v_x vs. shape index f: closed mark, maximum (broken line $v_x = 0.094\ f + 0.52$, $r = 0.19$): open mark, minimum (dotted line $v_x = 0.32\ f + 0.21$, $r = 0.38$): period of 0.33 μs.

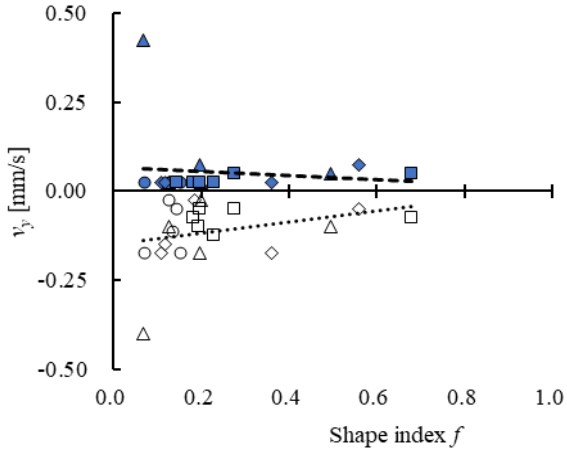

Fig. 3b: Velocity v_y vs. shape index f: closed mark, maximum (broken line $v_y = -0.058\ f + 0.66$, $r = 0.11$): open mark, minimum (dotted line $v_y = 0.16\ f - 0.15$, $r = 0.30$): period of 0.33 μs.

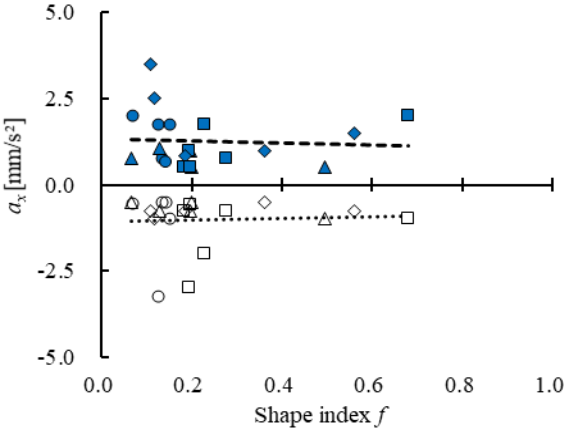

Fig. 4a: Acceleration α_x vs. shape index f: closed mark, maximum (broken line $\alpha_x = -0.27\ f + 1.3$, $r = 0.06$): open mark, minimum (dotted line $\alpha_x = 0.19\ f - 1.1$, $r = 0.04$): period of 0.33 μs.

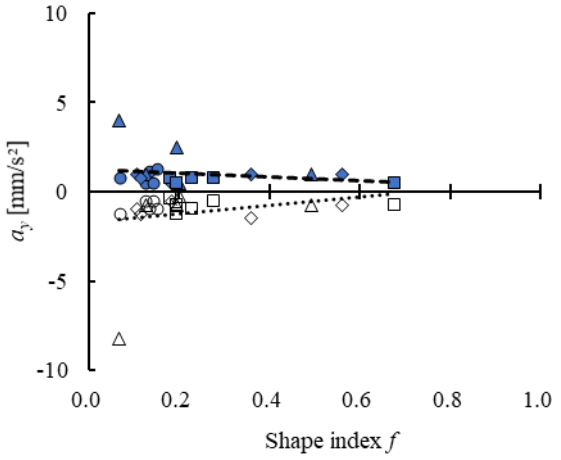

Fig. 4b: Acceleration α_y vs. shape index f: closed mark, maximum (broken line $\alpha_y = -1.1\,f + 1.2$, $r = 0.21$): open mark, minimum (dotted line $\alpha_y = 2.4\,f - 1.7$, $r = 0.23$): period of 0.33 μs.

While passing through the electric field, the movement of each cell is accelerated and decelerated. In the y direction, the minimum value (α_{ymin}) occurs before passing near the tip of the electrode. The maximum value (α_{ymax}) occurs after passing near the tip of the electrode. The range of fluctuation tends to decrease with increase of the shape index (Figs. 4a and 4b). The small absolute values in Fig. 4b correspond to those in Fig. 3b.

The acceleration of the y component is displayed in relation to the angle between the major axis of each cell and the direction of the main flow (0 degrees < θ < 180 degrees) in Fig. 5. The higher acceleration occurs around 90 degrees, which corresponds to the direction of the major axis of the cell perpendicular to the main flow direction.

The cumulative shifted distance (Δy) is displayed in relation to the angle between the major axis of each cell and the direction of the main flow (θ) in Fig. 6. The larger shifted distance occurs around 90 degrees, which corresponds to the direction of the major axis of the cell perpendicular to the main flow direction.

Fig. 7 shows the relationship between the shifted distance Δy and the shape index of each cell. The scattering of data decreases with increase of shape index. The tendency is similar to the tendency in Figs, 3b and 4b.

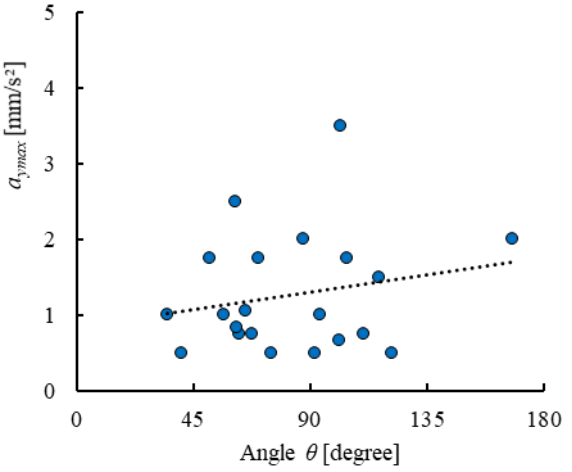

Fig. 5: Maximum value of acceleration α_{ymax} vs. angle θ: $a_{ymax} = 0.0051\,\theta + 0.84$, $r = 0.21$: period of 0.33 μs.

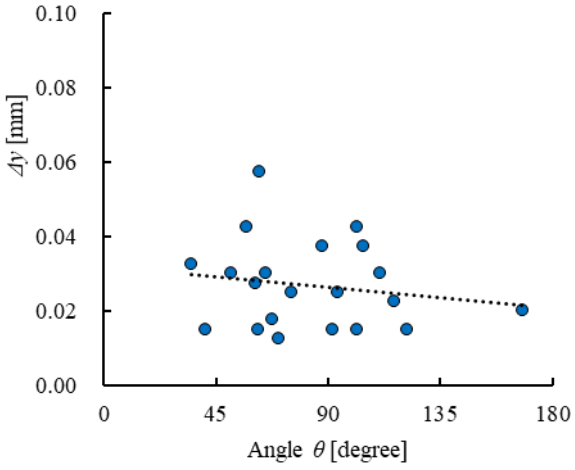

Fig. 6: Shifted distance Δy vs. angle θ: dotted line $\Delta y = 0.00006\,\theta + 0.032$, $r = 0.17$: period of 0.33 μs.

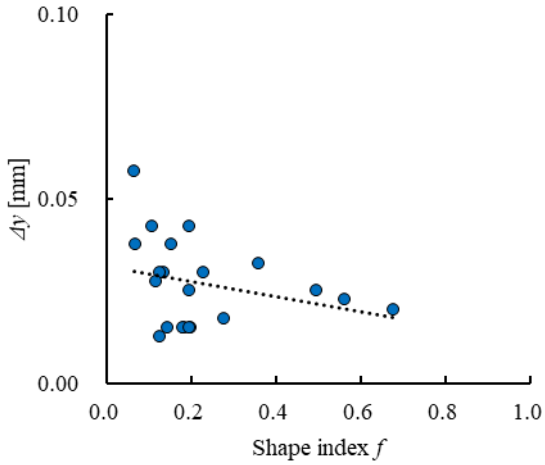

Fig. 7: Shifted distance Δy vs. shape index f: dotted line $\Delta y = -0.021\,f + 0.032$, $r = 0.28$: period of 0.33 μs.

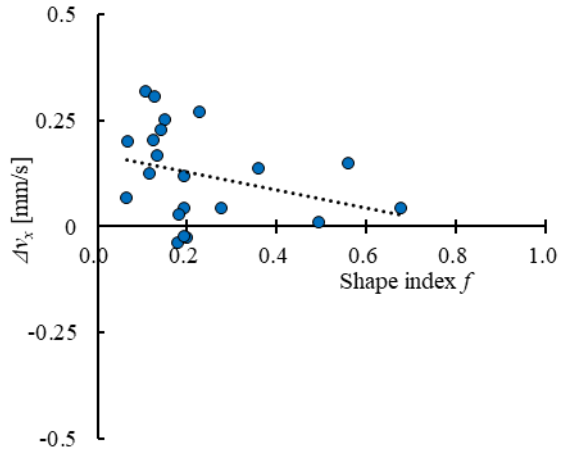

Fig. 8a: Velocity change Δv_x vs. shape index f: dotted line $\Delta v_x = -0.21\, f + 0.17$, $r = 0.31$: period of 0.33 μs.

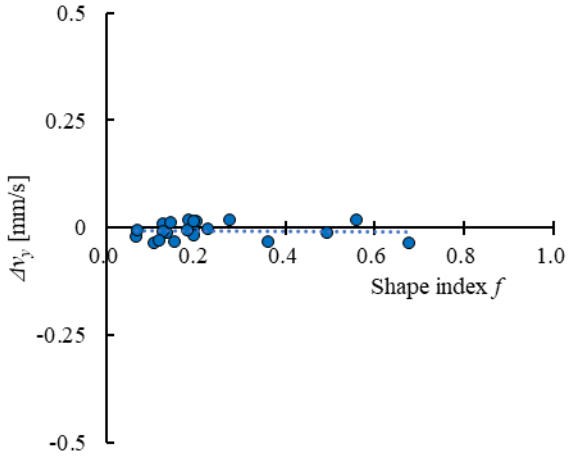

Fig. 8b: Velocity change Δv_y vs. shape index f: dotted line $\Delta v_y = -0.0061\, f - 0.0069$, $r = 0.05$: period of 0.33 μs.

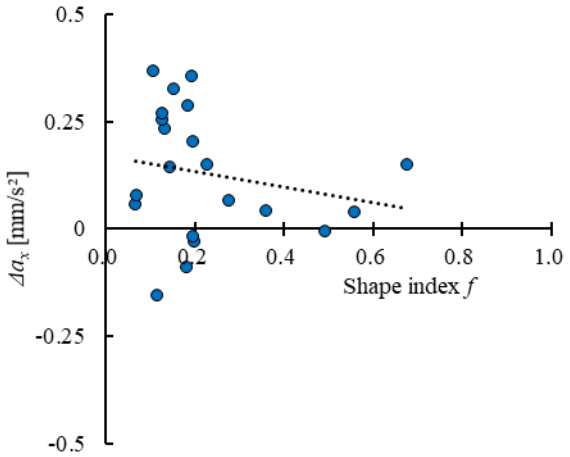

Fig. 9a: Acceleration change $\Delta \alpha_x$ vs. shape index f: dotted line $\Delta a_x = -0.18\, f + 0.17$, $r = 0.20$: period of 0.33 μs.

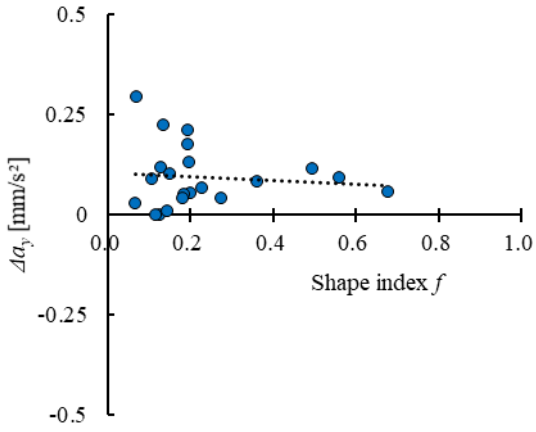

Fig. 9b: Acceleration change $\Delta \alpha_y$ vs. shape index f: dotted line $\Delta \alpha_y = -0.05\, f + 0.11$, $r = 0.11$: period of 0.33 μs.

Fig. 8 shows the velocity change related to the shape index. The negative value of Δv corresponds to the cell, of which the velocity after passing adjacent to the tip of the electrode is slower than that before passing adjacent to the tip of the electrode. The absolute value of Δv_y is small (Fig. 8b), because the absolute value of the y component of the velocity (v_y) is lower than that of the x component of the velocity v_x (Fig. 3). The positive values in Fig. 8a indicate that the velocities are higher after passing the electric field in most cells. The scattering of data decreases with increase of shape index (Fig. 8a).

Fig. 9 shows the acceleration change related to the shape index. The negative value of $\Delta \alpha$ corresponds to the cell, of which the acceleration after passing adjacent to the tip of the electrode is lower than that before passing adjacent to the tip of the electrode. The positive values in Fig. 9 indicate that the acceleration is higher after passing through the electric field in most cells. The scattering of data decreases with increase of shape index (Figs. 9a and 9b): period of 0.33 μs.

4. DISCUSSION

The micro flow channel is useful for sorting biological cells. Dielectrophoretic movement of cells through the micro flow-channel were investigated in previous studies [16, 17]. The dielectrophoretic force increases with the radius of a sphere (Eq. (1)), which is floating in the fluid. The moving cell experiences a the resistant force from the fluid.

Reynolds number (*Re*) is calculated by Eq. (5).

$$Re = \rho\, v\, h / \eta \qquad (5)$$

In Eq. (5), ρ is the density of the fluid [kg m^{-3}], v is the velocity [m s^{-1}], h is the distance [m] between the moving wall and the stationary wall, and η is the viscosity of the fluid [Pa s]. In the flow test in the present study, ρ, v, h, and η are 1×10^{3} kg m^{-3}, 1×10^{-3} m s^{-1}, 3.5×10^{-5} m, and 1.5×10^{-3} Pa s, respectively. Using these parameters, Re is calculated as 2×10^{-2}. Hence turbulent flow does not occur in the micro-channel. The cell receives viscous resistance from the fluid.

A sphere is symmetric. The movement of the sphere does not depend in its direction. The shape of the cell deviates from the sphere. The viscous resistance depends on the shape and angle of the moving cell. The specific angle of the cell could stabilize the movement of the flowing cell and reduce the viscous resistance. The movement of the flowing object depends on its rotation (cf. Magnus effect). The effect of rotation can be one of the reasons for the fluctuation of the movement of the cell. The dielectrophoretic effect could depend on the angle of the deformed cell. The acceleration of the cell movement along the main flow has been detected in the experiment of the present study (Fig. 4a). The cell movement perpendicular to the main flow, however, is easier to be used for cell classification than the movement parallel to the main flow. When the major axis of the cell is perpendicular to the flow, the resistance to the flow is large, and the effect of the force experienced by the electric field is also large.

Several kinds of forces can be applied to the flowing cell during its passage through the electric field in the flow channel: the resistant force to the movement of the flowing cell due to the flow of the medium, the resistant force due to the viscosity of the medium, and the dielectrophoretic force. When the cell deforms into an ellipsoid ($f > 0.4$), the viscous resistance can reduce the movement perpendicular to the flow direction. This mechanism can be applied to sorting cells according to their deformability.

The deformation of each cell during the movement along the flow can cause the change in the dielectrophoretic force passing through the electric field. The dielectrophoretic movement mainly depends on the shape index of the cell at the timing when the cell is passing near the tip of the electrode. The fluctuation in the dielectrophoretic movement of each cell relates to the fluctuation in the deformation of the cell.

The cell movement perpendicular to the flow of the medium depends on the location of the route through which the cell flows. The maximum movement perpendicular to the flow direction occurs for the route passing near the tip of the electrode. The shift distance depends on the path taken by the cell in the electric field, because a nonuniform electric field is necessary for dielectrophoretic movement. The cumulative shift distance (Δy) also depends on the velocity of the cell [18].

The gap in the z-direction, which is perpendicular to the x-y plane, is small (35 μm) in the flow channel of the present study. A nozzle type of guide at the upstream of the flow channel might be effective to adjust the initial position of the cell. For a more precise analysis, three-dimensional information of cell is necessary. In the present study, only the two-dimensional projected shape is analyzed. The rotation of the cell can display the change of the shape index. Therefore the effect of dielectrophoresis can vary by the rotation of the cell with the asymmetric shape.

5. CONCLUSION

The movement of each mouse myoblast cell flowing through the perpendicular electric field in the micro channel has been analyzed *in vitro*. The velocity change near the tip of the electrode is lower for a highly elongated cell. The maximum movement perpendicular to the main flow direction occurs when the major axis is perpendicular to the main flow direction.

ACKNOWLEDGEMENT

The authors thank Mr. Daisuke Hasegawa, and Mr. Takeru Noji for the help of the experiment.

REFERENCES

[1] Y, Guan, Y. Liu, H. Lei, S. Liu, F. Xu, X. Meng, M. Bai, X. Wang and G. Yang, "Dielectrophoresis Separation of Platelets Using a Novel Zigzag Microchannel", Micromachines, Vol. 11, No. 10, 890, 2020, pp. 1-15.

[2] S. Hashimoto, H. Sugimoto and H. Hino, "Effect of Couette Type of Shear Stress Field with Axial Shear Slope on Deformation and Migration of Cell: Comparison Between C2C12 and HUVEC", Journal of Systemics, Cybernetics and Informatics, Vol. 17, No. 2, 2019, pp. 4-10.

[3] Q. Wang, X. Zhang, D. Yin, J. Deng, J. Yang and N. Hu, "A Continuous Cell Separation and Collection Approach on a Microfilter and Negative Dielectrophoresis Combined Chip", Micromachines, Vol. 11, No. 12, 1037, 2020, pp. 1-13.

[4] S. Hashimoto, K. Kakishima and Y. Takahashi, "Cell Deformation Passing through Slit between Micro-Machined Surfaces in Vitro: Comparison among Cell Types", Proc. 23rd World Multi-Conference on Systemics Cybernetics and Informatics, Vol. 4, 2019, pp. 100-105.

[5] M. Heijazian, W. Li and N.T. Nguyen, "Lab on a Chip for Continuous-flow Magnetic Cell Separation", Lab on a Chip, Vol. 15, No. 4, 2015, pp. 959-970.

[6] H. Imasato and T. Yamakawa, "Measurement of Dielectrophoretic Force by Employing Controllable

Gravitational Force", Journal of Electrophoresis, Vol. 52, No. 1, 2008, pp. 1-8.
[7] Y. Takahashi, S. Hashimoto, H. Hino, A. Mizoi and N. Noguchi, "Micro Groove for Trapping of Flowing Cell", Journal of Systemics, Cybernetics and Informatics, Vol. 13, No. 3, 2015, pp. 1-8.
[8] C. Chen, X. Bai, Y. Ding and I.S. Lee, "Electrical Stimulation As a Novel Tool for Regulating Cell Behavior in Tissue Engineering", Biomaterials Research, Vol. 23, No. 1, 25, 2019, pp. 1-12.
[9] P.Y. Chu, C.H. Hsieh, C.R. Lin and M.H. Wu, "The Effect of Optically Induced Dielectrophoresis (ODEP)-Based Cell Manipulation in a Microfluidic System on the Properties of Biological Cells", Biosensors, Vol. 10, No. 6, 2020, pp.1-13.
[10] A. Shamloo, A. Yazdani and F. Saghafifar, "Investigation of a Two-step Device Implementing Magnetophoresis and Dielectrophoresis for Separation of Circulating Tumor Cells from Blood Cells", Engineering in Life Sciences, Vol. 20, No. 7, 2020, pp. 296-304.
[11] M. Sivaramakrishnan, R. Kothandan, D.K. Govindarajan, Y. Meganathan and K. Kandaswamy, "Active Microfluidic Systems for Cell Sorting and Separation", Current Opinion in Biomedical Engineering, Vol. 13, 2020, pp. 60-68.
[12] B. Zhu, W. Li, M. Zhu, P.L. Hsu, L. Sun and H. Yang, "Dielectrophoresis-Based Method for Measuring the Multiangle Mechanical Properties of Biological Cells", BioMed Research International, Vol. 2020, No. 5, 2020, pp. 1-9.
[13] Z. Çaglayan, Y.D. Yalçın and H. Külah, "A Prominent Cell Manipulation Technique in BioMEMS: Dielectrophoresis", Micromachines, Vol. 11, No. 11, 990, 2020, pp. 1-36.
[14] X. Xuan, B. Xu and D. Li, "Accelerated Particle Electrophoretic Motion and Separation in Converging-diverging Microchannels", Analytical Chemistry, Vol. 77, No. 14, 2005, pp. 4323-4328.
[15] P.N. Carlsen, Polydimethylsiloxane: Structure and Applications, Nova Science Publishers, 2020, pp. 29-94.
[16] Y. Takahashi, S. Hashimoto, M. Watanabe and D. Hasegawa, "Dielectrophoretic Movement of Cell around Surface Electrodes in Flow Channel", Journal of Systemics Cybernetics and Informatics, Vol. 16, No. 3, 2018, pp. 81-87.
[17] S. Hashimoto, T. Noji, H. Yonezawa and Y. Endo, "Effect of Shape of Cell on Dielectrophoretic Movement in Flow Channel", Proc. 12th International Multi-Conference on Complexity, Informatics and Cybernetics, Vol. 2, 2020, pp. 37-42.
[18] S. Hashimoto, D. Hasegawa, Y. Takahashi and R. Matsuzawa, "Design of Flow Channel with Surface Electrodes to Detect Dielectrophoretic Movement of Floating Myoblast", Proc. 23rd World Multi-Conference on Systemics Cybernetics and Informatics, Vol. 4, 2019, pp. 94-99.